



# Bamboo Leaf Flavonoids Extracts Alleviate Oxidative Stress in HepG2 Cells via Naturally Modulating Reactive Oxygen Species Production and Nrf2-Mediated Antioxidant Defense Responses

Yue Yu, Zhanming Li , Guangtian Cao, Shudan Huang, and Hongshun Yang 

**Abstract:** In this study, bamboo leaf flavonoids extracts (BFE) were employed to alleviate oxidative stress induced by oleic acid in HepG2 cells. Biochemical indexes, intracellular reactive oxygen species production, lipid droplets accumulation, antioxidant enzymes production, and mitochondrial membrane potential were determined to show the alleviation performance of BFE intervention ( $P < 0.05$ ). Importantly, the results of qRT-PCR and western blot determination indicated that BFE intervention upregulated the expression of Nrf2/HO-1/NQO1 to initiate the antioxidant defense response for counteracting oxidative stress ( $P < 0.05$ ). Moreover, mitochondrial membrane potential-mediated apoptosis and FOXO signaling pathway initiation caused by BFE intervention may together contribute to oxidative stress alleviation in HepG2 cells. In conclusion, these findings suggested that BFE intervention upregulated related antioxidant defense responses for preventing cells from oxidative damage.

**Keywords:** antioxidant defense responses, bamboo leaf, flavonoids, oleic acid, oxidative stress

**Practical Application:** In this study, bamboo leaf flavonoids extracts intervention upregulated related antioxidant defense responses for preventing cells from oxidative damage. These findings in bamboo leaf extracts antioxidants are a promising and innovative subject with practical applications to enhance the development of bamboo leaf extracts functional products in the food industry.

## Introduction

Dietary patterns with high energy and fat density produce numerous reactive oxygen species (ROS) production and consequently induced oxidative stress associated with many diseases, including cancers and cardiovascular diseases (Kubben & Misteli, 2017). Oxidative stress is an unbalance status between free radicals and antioxidant activities. Oxidative damage of the biomolecules is associated with free radicals, inducing various oxidative products to generate cell damage (Manach et al., 2017; Rani, Deep, Singh, Palle, & Yadav, 2016). As reported in previous researches, natural antioxidants from the plants play a vital role to prevent oxidative stress and reduce ROS production, which has been utilized to depress or alleviate the oxidative damage and related diseases (Ristow, 2014). Research interest in natural plant antioxidants is promising and innovative subject with practical applications, providing the nutritional knowledge of functional ingredients from plants (Girgih et al., 2015; Nwachukwu, Udenigwe, & Aluko, 2016).

Some active compound-enriched plant extracts have been proposed to alleviate cell damage for sustaining proper cell function (Ayyash et al., 2018). It was considered that dietary raspberry provided a promising effect to attenuate obesity in mice induced by high-fat diet (Wu et al., 2018). Moreover, lingonberry extracts were suggested as a coadjuvant for preventing diabetes (Reichert et al., 2018). It was also reported that rosemary aqueous extracts with anti-inflammatory effects were able to attenuate oxidative stress produced from arthritis (de Almeida Gonçalves et al., 2018).

Upregulation of intracellular antioxidant enzymes generation by diverse signaling pathways triggered by antioxidant defense response is an alternative strategy for preventing oxidative damage (Lee et al., 2015). Particularly, it is commonly recognized that Nrf2-mediated pathway activation is the main mechanism for cancer cells to increase their antioxidant proteins (Sporn & Liby, 2012). Expression of HO-1 and NQO1, regulated by Nrf2, are together able to form the antioxidant defense system to prevent the cell from oxidative damage (Wardyn, Ponsford, & Sanderson, 2015). Jaja-Chimedza et al. (2018) suggested that the Nrf2 pathway was initiated by diet moringa seed extracts for improving anti-inflammatory and metabolic health. Therefore, the regulation of Nrf2, HO-1, and NQO1 expression is studied to understand the antioxidant defense response triggered by ROS production. Also, the related antioxidant defense responses, such as the release of antioxidant proteins and signaling pathways initiation, are also needed to clarify.

JFDS-2018-1926 Submitted 11/28/2018, Accepted 3/16/2019. Author Yu is the Huzhou Vocational and Technical College, Huzhou 313000, PR China. Authors Yu, Li, Cao, and Huang are with the Dept. of Food Science, China Jiliang Univ., Hangzhou 310018, PR China. Authors Li and Yang are with the Food Science and Technology Programme, Dept. of Chemistry, National Univ. of Singapore, Singapore 117543, Singapore. Direct inquiries to author Zhanming Li (E-mail: lizhanming@jlu.edu.cn).

Dietary plant flavonoids supplementation is frequently utilized to reduce ROS production and intervene oxidative damage effectively, promoting human health (Fatokun, Tome, Smith, Darlington, & Stone, 2015). It was reported that flavonoids from *Averrhoa carambola* L. fruit produced higher ABTS radical scavenging activity than L-ascorbic acid (Yang, Xie, Jia, & Wei, 2015). Apoptosis in HepG2 cells was induced by C-glycosyl flavonoids via JNK and p38 kinases activation and ERK1/2 kinase inactivation (Yuan et al., 2013). Moreover, C-glycosyl flavonoids also triggered HeLa cells apoptosis and prevented erythrocytes from oxidative damage through downregulating Bcl-2 expression and upregulating caspase-3 protein production (Girish, Kumar, & Prasada Rao, 2016).

Bamboo leaf flavonoids extracts (BEE) have caused considerable attention for their bioactivities, such as antioxidant, antibacterial, antitumor, anti-inflammatory, antidiabetic diseases, anti-aging activities, and so on (Nirmala, Bisht, Bajwa, & Santosh, 2018). Gong et al. (2014) suggested that bamboo flavonoids produced promising free radical scavenging activity. It was also considered that bamboo flavonoids were used to depress the proliferation of cancer cells and inactivate the inflammatory response mediated by NF- $\kappa$ B signal pathways (Thangaraj & Vaiyapuri, 2017).

In China, bamboo leaf antioxidants extracted from *Phyllostachys Siet. Et Zucc* leaf have been authorized by the National Health Commission of China as food antioxidant additives (National Health Commission, 2014). It was considered that the specific flavonoid compounds of bamboo leaf extracts were flavonoids, lactones, and phenolic acids (Zhang, Jiao, Liu, Wu, & Zhang, 2008; Wu et al., 2012). However, rare research on BFE was studied to clarify the alleviation for the high fat-induced oxidative stress. In this work, water-soluble BFE was used to observe oxidative stress alleviation in HepG2 cells. The aim of the current study was to evaluate whether BFE intervention alleviates oleic acid (OA)-induced oxidative stress in HepG2 cells. Moreover, ROS production regulation and related antioxidant defense responses initiation were also performed.

## Materials and Methods

### Materials and agents

A laboratory grinding mill was used to grind the bamboo leaf samples and water-soluble extraction was dried by freeze drying. The solid was collected as BFE samples and used for the experiments. HepG2 cells were obtained from the Shanghai Institutes for Biological Sciences (Shanghai, China). Glutathione peroxidase (GSH-Px), lactate dehydrogenase (LDH), triglyceride (TG), malondialdehyde (MDA), catalase (CAT), and total antioxidant capacity (T-AOC) kits were used to determine the biochemical indexes (Nanjing Jiancheng Bioengineering Inst., Nanjing, China). Oil Red O, Folin-Ciocalteu phenol reagent, gallic acid, hematoxylin, 3-(4,5-dimethyl-2-thiazolyl)-2,5-diphenyl-2H-tetrazolium bromide (MTT), isopropanol, ( $\pm$ )-catechin, OA, and 2,7-dichlorofluorescein diacetate (DCF-DA) were purchased from Sigma Chemical Co., Ltd. (St. Louis, MO, USA). HiScript Reverse Transcriptase (RNase H), 5 $\times$  HiScript Buffer, 50 $\times$  ROX Reference Dye 2, and SYBR Green Master Mix were obtained from Vazyme Biotech (Nanjing, China). Taq Plus DNA Polymerase, dNTP, and DL2000 DNA Marker were obtained from Tiangen (Tiangen Biotech Co., Ltd., Beijing, China). Fetal bovine serum (FBS), TRIzol reagent, trypsin, and culture medium RPMI-1640 were obtained from Gibco (Gibco/BRL Life Technologies, Grand Island, NY, USA). Culture dishes and cell culture

flasks (Corning Costar Corp., Cambridge, MA, USA) were used for cell culture. Antibodies for Cyt C, Nrf2, and HO-1 were purchased from Tiangen Biotech Co., Ltd. All other reagents were of analytical grade or the best grade available.

### BFE analysis

**Total polyphenols contents.** Novel Folin-Ciocalteu assay was performed to determine the total polyphenols contents (TPC) according to previous studies (Chen et al., 2018; Xu, Jin, Peckrul, & Chen, 2018). The samples were determined at 765 nm according to the standard curve of gallic acid. Milligrams gallic acid equivalent (GAE) per gram of dry materials basis (mg GAE/g dmb) was used to express the results.

**Total flavonoid content.** Total flavonoid content (TFC) was determined by a standard curve of ( $\pm$ )-catechin. In brief, a standard curve of ( $\pm$ )-catechin solution (0.2 mg/mL, and 0, 25, 50, 75, 100, and 125  $\mu$ L) was prepared, and the volume of the solutions was set to 500  $\mu$ L with 60% ethanol-water solution. Then, an aluminum nitrate solution (10%, 30  $\mu$ L) was added into the mixture in 6 min after the addition of sodium nitrite solution (5%, 30  $\mu$ L). After 6 min, sodium hydroxide solution (4%, 400  $\mu$ L) was used to quench the reaction and then ethanol-water solution (40  $\mu$ L) was added. Milligrams of ( $\pm$ )-catechin equivalent (CE) per gram of dry materials basis (mg CE/g dmb) was employed to express the TFC results.

**Ultra performance liquid chromatography (UPLC) analysis.** UPLC analysis was proposed to determine the specific compounds (orientin, isorientin, vitexin, and isovitexin) according to the following procedures. BFE samples were dissolved into methanol solution (1 mg/mL) and the solution was vortex-mixed and centrifuged for 10 min (8,000  $\times$  g, 4  $^{\circ}$ C). The filtered supernatant (1.0  $\mu$ L) was injected for analysis. Waters ACQUITY UPLC BEH C8 (150 mm  $\times$  2.1 mm, 1.7  $\mu$ m) column was used for the UPLC analysis and the analytes were determined at 340 nm. Mobile phase A consisting of 0.1% aqueous phosphoric acid and mobile phase B containing 100% acetonitrile (A:B = 82:18) were used for the gradient elution at a flow rate of 0.21 mL/min. Standard mixtures of chlorogenic acid, caffeic acid, isorientin, coumaric acid, orientin, isovitexin, vitexin, ferulic acid, and coumaric acid (purity >97%) were used to determine the components of BFE samples.

### Cell culture

HepG2 cells were maintained in RPMI-1640 with 10% heat-inactivated FBS (100 U/mL penicillin and streptomycin added) and incubated at 37  $^{\circ}$ C with 5% CO<sub>2</sub>. The culture process followed was in accordance with the study of Ferlazzo et al. (2016). After several culture processing, the solution of the cells with the concentration of 6  $\times$  10<sup>5</sup> cells/mL was incubated on the microplates. Blank solutions, different OA solutions, and BFE solutions were used for incubation to determine the cell viability and biochemical indexes. The harvested cells were also used to determine ROS production and others.

In this study, five treatments were presented as follows. The cells incubated with medium containing OA for 24 hr were treated as OA24 group. The cells incubated with a normal medium for 24 hr were treated as a control group. The cells incubated with medium containing OA for 12 hr and then incubated with a normal medium for 12 hr were treated as OA12+C12 group. The cells incubated with medium containing OA for 12 hr and then incubated with medium containing BFE for 12 hr were treated as OA12+BFE12 group. The cells incubated with

medium containing OA and BFE mixture for 24 hr were treated as (OA+BFE)24 group.

### Cell viability assay

Cell viability assays were determined using MTT experiments as previous researches (Ferlazzo et al., 2016). In brief, treated HepG2 cells were seeded onto 96-well plates ( $5 \times 10^4$  cells/well) in triplicate for MTT assay. Twenty-four hours after plating, OA solutions (0 to 1.6 mM) were added into the wells for incubation. Ten microliters MTT solution was added after the incubation. The medium was removed after 4-hr incubation and cell solution was determined at 570 nm using a microplate reader. Other treatments with OA and/or BFE solutions were also proposed as the protocols above. Results were expressed as percentages of cell viability and the control samples were set as 100%. OA concentration and BFE concentration were both optimized by MTT assays.

### Biochemicals assay

LDH and TG levels of supernatant were determined according to the kits instructions. MDA production increased if the samples were treated to cause oxidative stress. Antioxidants were involved with oxidative stress alleviation by means of suppression and removal of the free radicals. The performance can be described using the increase in CAT and GSH-Px production during the intervention. MDA, CAT, GSH-Px, and T-AOC levels were determined according to the ELISA kits instructions.

### Oil red O staining

Cell samples were fixed for 15 min followed by water wash. Oil Red O was used for cell staining for 10 min after 60% isopropanol immersion. Mayer hematoxylin stain was used for several minutes with oil blackening for 3 min (Cao, Tao, Xin, Li, & Zhou, 2018). The treated samples were observed using the Olympus biological microscope (BX53; Olympus, Tokyo, Japan).

### Intracellular ROS production

After digestion with 0.25% pancreatin, the harvest cells were concentrated for 5 min at  $1200 \times g$  and then the supernatant was removed. PBS was used to resuspend the cells and then the solution was concentrated again. The diluted DCF-DA solution, used as fluorescence probe, was added into the wells and then incubated with the cells at 37 °C (20 min). Serum-free medium was used to incubate the cells as negative control. The solutions were mixed every 3 min and then washed triple with the serum-free medium. ROS production was determined with flow cytometry (CytoFLEX, Beckman, Pasadena, CA, USA).

### Mitochondrial membrane potential

JC-1 assay kit was employed to observe the mitochondrial membrane potential of cells according to the instructions and determined by the ratio of red/green fluorescence probe. Cells were cultured and treated with OA or BFE solutions and then the samples were washed twice with phosphate buffer solution (PBS). JC-1 working solution with serum-free medium (5 µg/mL) was added to stain for 40 min. Flow cytometry was used to determine the fluorescence after washing twice with PBS.

### qRT-PCR analysis

Total RNA was isolated and qRT-PCR was performed with an ABI QuantStudio 6 Flex system (ABI, Carlsbad, CA, USA). Forward and reverse primer sequences of Nrf2, NQO1, and HO-1 designed using the Primer Premier 6 software (Premier Biosoft,

USA) are shown in Table S1. Results of mRNA quantity were calculated by the meaning of the  $2^{-\Delta\Delta Ct}$  method. All samples were performed in triplicate and the average values were analyzed.

### Western blot analysis

Western blot analysis was employed to determine the relative expression of Cyt C, Nrf2, and HO-1. The control group, OA24 group, and (OA+BFE24) group were used for this analysis to explore changes in upstream signaling pathway protein expression according to the reference (Kim, Ahn, & Je, 2016). Briefly, the lysed HepG2 cells solution for different treatments was centrifuged at  $12,000 \times g$  at 4 °C for 20 min to remove the insoluble material. The separated proteins via SDS-PAGE (10%) were transferred to a PVDF membrane. After blocking, the PVDF membrane was incubated with anti-Cyt C, anti-Nrf2, and anti-HO-1 at 4 °C overnight. After that, horseradish peroxidase-labeled secondary antibody was used to incubate the washed membrane for 2 hr. ECL assay kit (Thermo Scientific) was employed to determine the blots.

### Autophagosomes observation

The cells were fixed with glutaraldehyde and osmium tetroxide followed by the dry processing using ethanol solution at different concentrations (50%, 70%, 80%, 90%, 95%, and 100%). Finally, the stained embedding slides were photographed under a transmission electron microscope (HT-7700; Hitachi, Japan).

### Statistical analysis

A one-way ANOVA model (SPSS 17.0) was employed to observe the differences between treatments. Statistically significant differences were determined when  $P < 0.05$ . Entire test was in triplicates and the mean value  $\pm$  standard deviation was reported for each data analysis.

## Results and Discussion

### BFE analysis

TPC and TFC concentrations of water-soluble BFE samples were determined and results showed the TPC with the concentration of  $79.93 \pm 0.31$  mg GAE/g dwb and TFC with the concentration of  $78.83 \pm 0.23$  mg CE/g dwb. As reported, the major functional components of bamboo leaf extract are flavone C-glycosides, including orientin, isoorientin, vitexin, and isovitexin, which were used as markers to characterize the commercial bamboo leaf products (Wu et al., 2012; Yang et al., 2017). UPLC results (Figure S1) presented that concentration of chlorogenic acid, caffeic acid, isoorientin, coumaric acid, orientin, isovitexin, vitexin, and ferulic acid was 3.878, 3.373, 14.776, 2.489, 4.97, 4.204, 2.825, and 2.736 mg/L, respectively.

### Cell damage model

It has been commonly considered that OA can be employed to develop the cell damage model and determined by cell viability. Herein, to test the optimized OA concentration, a series of OA solutions were presented for cell viability observation. It was clear that different OA concentrations can be subjected to tune cell viability. As shown in Figure 1A, compared with the control group, OA-treated groups with a concentration of 0.4 mM and above produced significantly different cell viability for 12-hr incubation ( $P < 0.05$ ). The cell viability was decreased by nearly 30% when the cells were treated with 0.4 mM and above OA for 12 hr indicating the obvious cytotoxic effect. In particular, differences

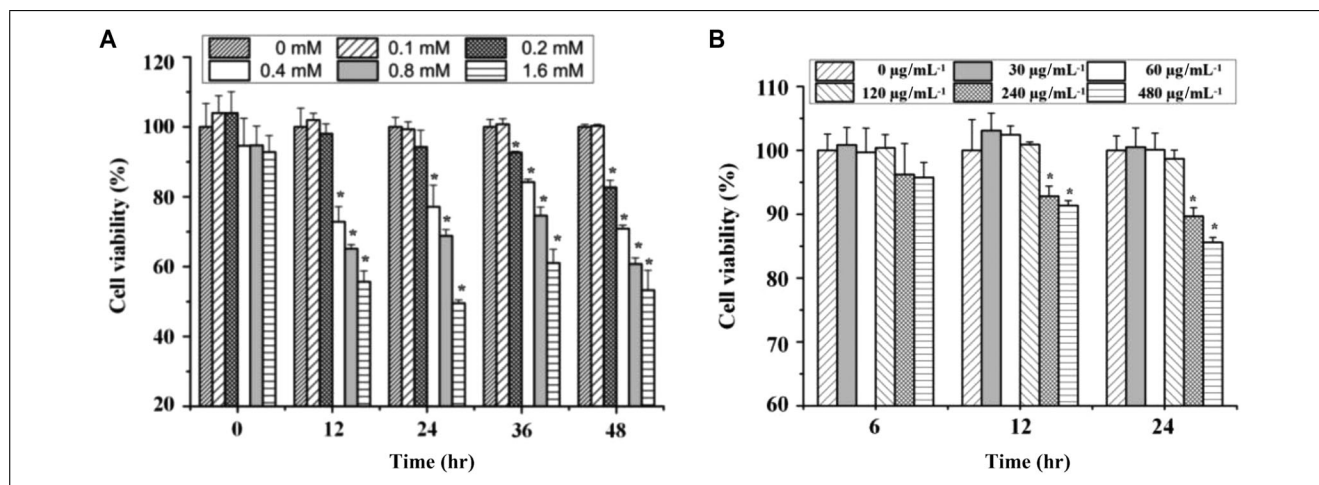


Figure 1—(A) Cell viability of different concentrations of OA (0 to 1.6 mM) for 0 to 48-hr incubation. (B) Cell viability of BFE addition at different concentrations (0 to 480 µg/mL) for 6-, 12-, and 24-hr incubation. The cell viability of the control samples in (A) and (B) were both set as 100%. \*Significant differences of the cell viability between the treated samples and the control samples ( $P < 0.05$ ).

were produced when the cells were treated with 0.2 mM OA for 36-hr incubation, indicating the cell damage ( $P < 0.05$ ), while no difference was produced for 24-hr incubation ( $P > 0.05$ ). Considering the effective cell damage without cytotoxic effect (Li et al., 2018), OA solution with the concentration of 0.2 mM was reasonably proposed as the treated concentration for the OA-induced cell damage model.

To observe the appropriate concentration, we performed the cell viability when treated with BFE at concentrations ranging from 0 to 480 µg/mL. It was indicated that the side effect was produced when HepG2 cells were treated with BFE samples at concentrations above 240 µg/mL (Figure 1B). BFE samples at a concentration below 120 µg/mL induced no difference in cell viability during 24-hr incubation ( $P > 0.05$ ). As mentioned above, 120 µg/mL BFE samples can be acted as the treated concentration for the alleviation.

We also observed LDH and TG production for the determination of the OA-induced cell damage model. As shown, the OA-treated cells were incubated for 12 and 24 hr, respectively. Compared with control samples, LDH and TG production had obtained a significant increase ( $P < 0.05$ ). The LDH production (Figure 2A) of the samples treated with 0.2 mM OA was increased by 150%, whereas the TG production (Figure 2B) was increased by 100% ( $P < 0.05$ ). It was indicated that 0.2 mM OA can be optimized as the damage concentration. Also, a significant difference in ROS production was determined between the control and OA-treated groups ( $P < 0.05$ ), acting as a sign of oxidative stress. Herein, we observed that ROS production was increased (Figure 2C) along with the increase in the OA concentration.

As mentioned above, compared with control samples, OA at the concentration of 0.2 mM and BFE at the concentration of 120 µg/mL presented the appropriate difference on the cell viability, TG, LDH, and ROS production during the 24 hr cell culture. Therefore, these parameters were suggested to propose the optimized cell damage model for the follow-up experiments.

### Biochemicals assay

Biochemicals including TG, LDH, MDA, CAT, GSH-Px, and T-AOC were determined to describe the cellular oxidation state and alleviation performance involved with BFE addition. As shown in Figure 3A and 3B, we can easily indicate that TG and MDA production increased dramatically due to 24-hr OA incuba-

tion ( $P < 0.05$ ). TG and MDA generation significantly decreased when the samples were incubated with medium containing OA for 12 hr and then incubated for another 12 hr without OA ( $P < 0.05$ ). Moreover, if the damaged samples with 12-hr OA incubation were further incubated with a medium containing BFE, the oxidative damage was further alleviated ( $P < 0.05$ ), and TG and MDA production further decreased to the control level ( $P > 0.05$ ).

Generally, LDH release in the surrounding medium is associated with cytotoxicity. As in Figure 3C, OA24 group presented the highest LDH generation indicating the abnormal oxidative stress state. Extracellular LDH production produced from the disrupted plasma membrane indicated the cytotoxicity of OA intervention. Compared with control samples, LDH production of OA12+BFE12 and (OA+BFE)24 groups decreased due to the addition of BFE ( $P < 0.05$ ). No difference was observed between OA12+BFE12 and (OA+BFE)24 groups ( $P > 0.05$ ). Although significant differences between the control and OA12+BFE12 groups were observed, LDH production enormously decreased compared with that of OA24 group ( $P < 0.05$ ).

It is reported that living cells contain a large number of antioxidant enzymes and CAT and GSH-Px production has been frequently employed to describe the cellular oxidative stress state (Wang et al., 2016). As shown in Figure 3D and 3E, cells with 24-hr OA incubation obtained the lowest CAT and GSH-Px production, showing the OA-induced oxidative damage ( $P < 0.05$ ). Also, cells with the control 12-hr or BFE 12-hr incubation can be employed to alleviate the decrease in CAT and GSH-Px levels ( $P < 0.05$ ). Furthermore, the performance was approximative between OA12+BFE12 and (OA+BFE)24 groups ( $P < 0.05$ ).

When the cells were in the oxidative stress state, antioxidant defense responses can be initiated by many antioxidants through different pathways (Chandel, 2015; Ristow, 2014). The T-AOC level can be used as an indicator to show oxidative stress (Figure 3F). OA incubation has significantly decreased T-AOC level of cells ( $P < 0.05$ ). OA12+C12 and OA12+BFE12 groups supported the same trend as CAT and GSH-Px productions. However, the performance of (OA+BFE)24 group was better than that of OA12+BFE12 group ( $P < 0.05$ ), indicating the involvement of other antioxidant enzymes or small molecules antioxidant can increase the antioxidant activities for maintaining the proper function (Schieber & Chandel, 2014).



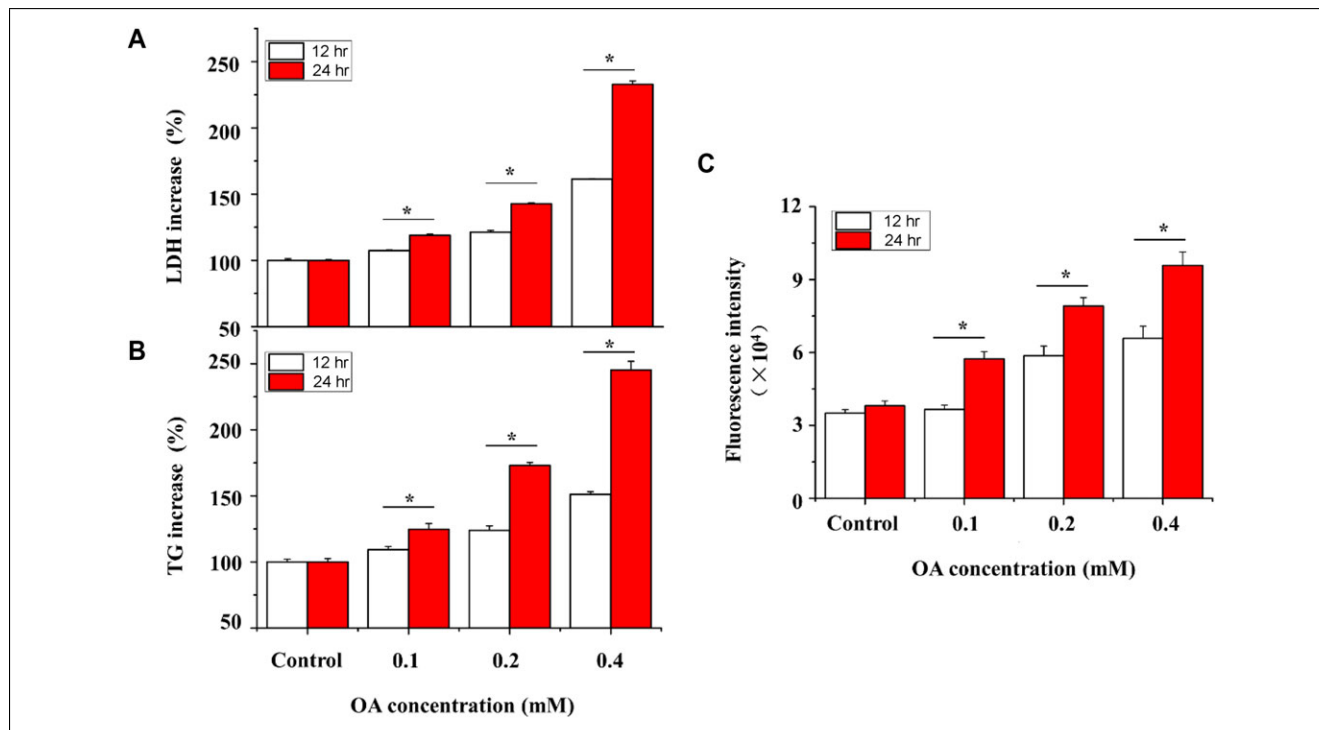


Figure 2—LDH (A) and TG (B) change in HepG2 cells incubated with OA solution (0, 0.1, 0.2, and 0.4 mM) for 12 and 24 hr. ROS production (C) was determined by fluorescence intensity. \*Significant difference between the 12-hr incubation samples and 24-hr incubation samples ( $P < 0.05$ ).

### Oil Red O staining

In agreement with biochemicals, the results of Oil Red O staining (Figure 4) also showed the same trend. Highest lipid droplet accumulation emerging from OA24 group (Figure 4A and B) discovered that the oxidation and impairment were able to generate high ROS production ( $P < 0.05$ ). Compared with OA24 group, the removal of OA played a pivotal role in the reduction of lipid droplets accumulation (Figure 4C). Recently, it is reported that the accumulation of lipid droplets contributed to the growth, proliferation, and metastasis of cancer cells (Menard et al., 2016). The very fast decrease in lipid droplet accumulation in this study was considered as a response of the BFE intervention (Figure 4D and E), underlining the importance of the antioxidant defense response. In support of this, it was further considered that OA24 group recognized the highest ROS production compared with other treatments (Figure 5).

### Intracellular ROS production

It is stressed that ROS production is often associated with the oxidative stress, and an increase in ROS production within cells indicates that the damage signaling occurred (West & Shadel, 2017). It has been revealed that high levels of ROS production are still involved with oxidative damage even to induce cell death (Mittal, Siddiqui, Tran, Reddy, & Malik, 2014). Thus, ROS production within the threshold allows cells to maintain the proper function, and steady-state ROS level is determined by the balance between ROS production and ROS scavenging (Schieber & Chandel, 2014).

Our observations were also in line with previous research that high ROS production was associated with cellular oxidative stress (Mittal et al., 2014). As shown in Figure 5A to 5F, ROS production of OA24 samples was the highest compared with that of other treatments ( $P < 0.05$ ). Moreover, when the OA stim-

ulation was removed, ROS production of OA12+C12 samples was lower than that of OA24 samples ( $P < 0.05$ ). Furthermore, OA12+BFE12 samples exhibited the lowest ROS production ( $P < 0.05$ ). Compared with control samples, (OA+BFE)24 group obtained the adjacent ROS level (Figure 5F). It was suggested that BFE intervention effectively decreased ROS production caused by OA intervention. ROS production using OA24 and OA12+C12 treatments was higher than that of other treatments ( $P < 0.05$ ). When BFE intervention was introduced, ROS production was dramatically decreased ( $P < 0.05$ ) indicating the oxidative stress alleviation. Fluorescence images showed in Figure 5G to 5K also suggested that OA24 group samples presented the highest ROS production indicating the cell damage, while BFE intervention decreased the fluorescence intensity effectively. Results of HepG2 cells with high ROS production causing oxidative stress were alleviated properly by BFE intervention and the introduced steady-state ROS level was helpful for sustaining normal function.

### Mitochondrial membrane potential

As the main source of cellular ROS production, mitochondria's proper function is critical for regulating cellular signaling. Change of mitochondrial membrane potential, as an important intracellular signal, can act as a signal for the whole cell to initiate antioxidant defense systems when the cell is under oxidative stress (Chandel, 2015). As shown in Figure 6A to 6E, the mitochondrial membrane potential of OA24 samples dramatically decreased compared with that of control samples ( $P < 0.05$ ), indicating the change in the cell's steady state and function. Compared with the control group, the mitochondrial membrane potential of (OA+BFE)24 and OA12+BFE12 groups lowered to a significant extent ( $P < 0.05$ ).

As shown in Figure 5F and 6E, the change rate of ROS production was approximately 10 times than that of mitochondrial

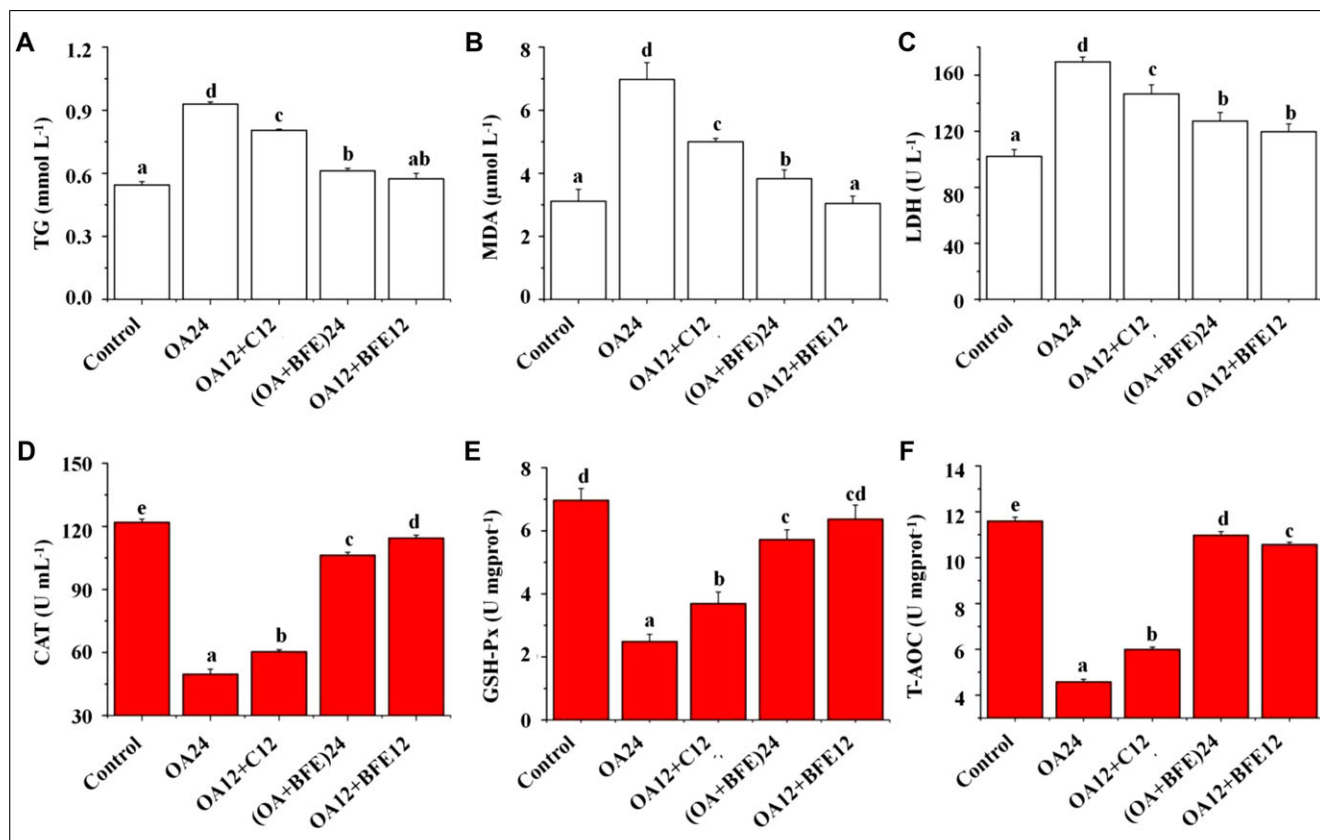


Figure 3—Biochemical assay of the treated HepG2 cells samples to present TG (A), MDA (B), LDH (C), CAT (D), GSH-Px (E), and T-AOC (F). Letters a to e represented the significant difference between the treated samples and the control samples ( $P < 0.05$ ).

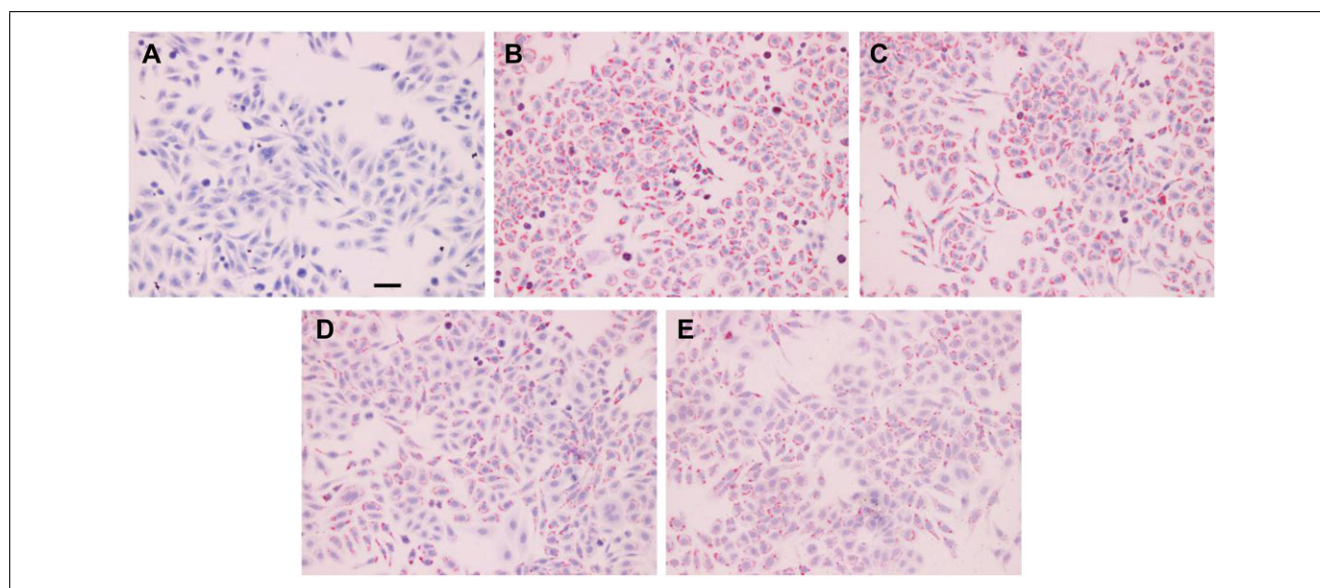


Figure 4—Images of the treated HepG2 cells after Oil Red O staining, the control group (A), OA24 group (B), OA12+C12 group (C), (OA+BFE)24 group (D), and OA12+BFE12 group (E). The blue part represented the nucleus and the red represented the lipid droplets. The scale bar was 50 μm.

membrane potential after OA24 incubation. After BFE intervention, the change of ROS production was also more significant than that of mitochondrial membrane potential. These results indicated that ROS production was more sensitive to oxidative damage than mitochondrial membrane potential. Importantly, as reported, the balance of mitochondrial membrane potential contributes to sus-

tain the proper cell function (Chandel, 2015). These findings in the current study present the oxidative stress alleviation of the BFE intervention and are associated with the effective modulation of mitochondrial membrane potential and high ROS production.

Improvement of mitochondrial membrane potential may contribute to the release of regulatory proteins, such as cytochrome

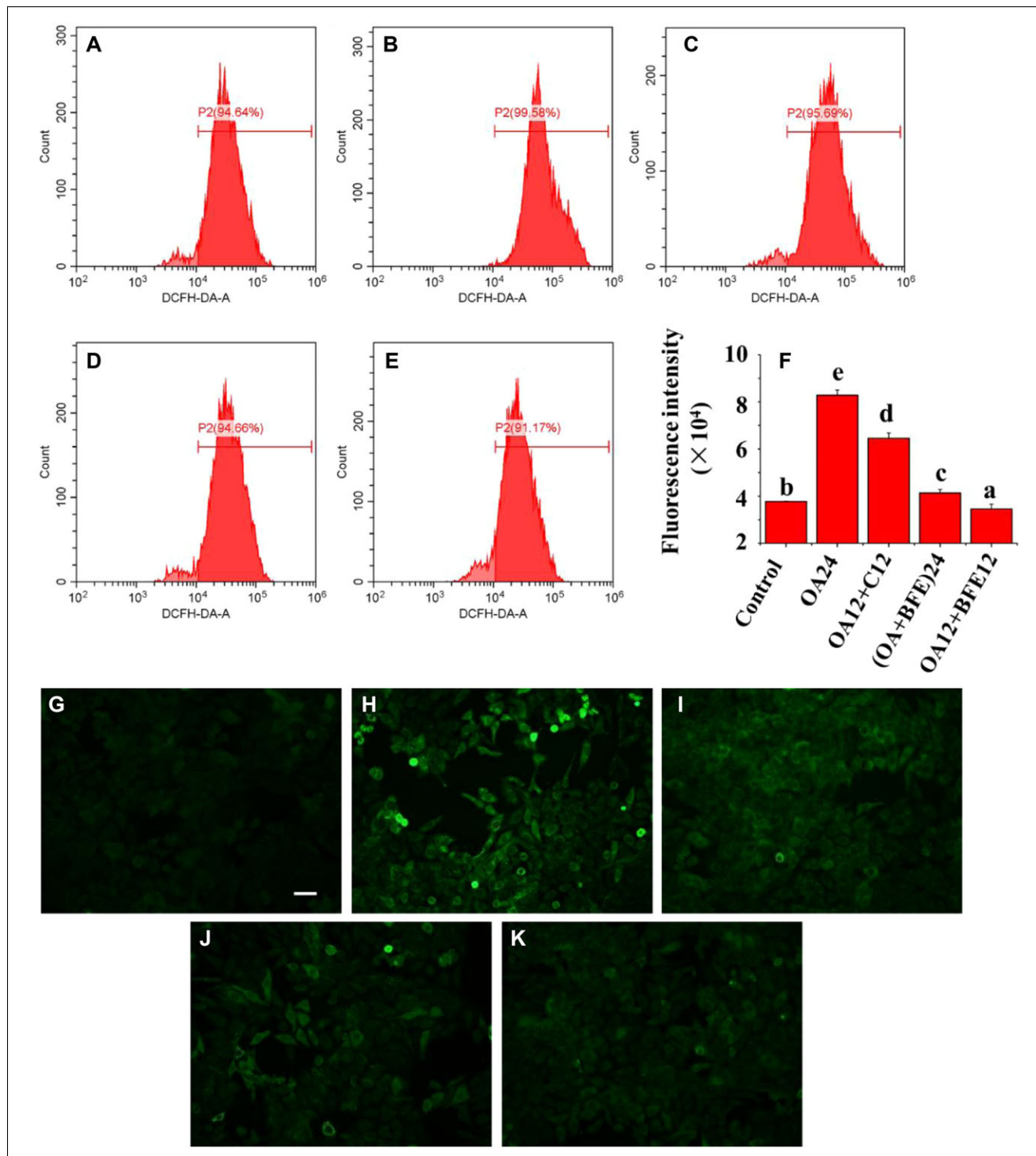


Figure 5—Intracellular ROS for the control group (A), OA24 group (B), OA12+C12 group (C), (OA+BFE)24 group (D), and OA12+BFE12 group (E). ROS production (F) and fluorescence photos for the control group (G), OA24 group (H), OA12+C12 group (I), (OA+BFE)24 group (J), and OA12+BFE12 group (K). The scale bar was 50  $\mu$ m.

C (Cyt C; Martínez-Reyes et al., 2016). Importantly, Cyt C was also associated with the initiation of apoptosis. In order to explore the potential regulatory mechanism, we observed the expression of Cyt C using western blot. As shown in Figure S2, the Cyt C expression of OA24 samples was dramatically increased and decreased by BFE intervention ( $P < 0.05$ ), indicating the alleviation of the apoptosis induced by the BFE intervention. It was

concluded that the mitochondrial membrane potential-mediated apoptosis pathway contributed to the oxidative stress modulation during the BFE intervention.

#### Principal components analysis

Principal components analysis and cluster analysis were employed to describe the variance of different groups. Control,

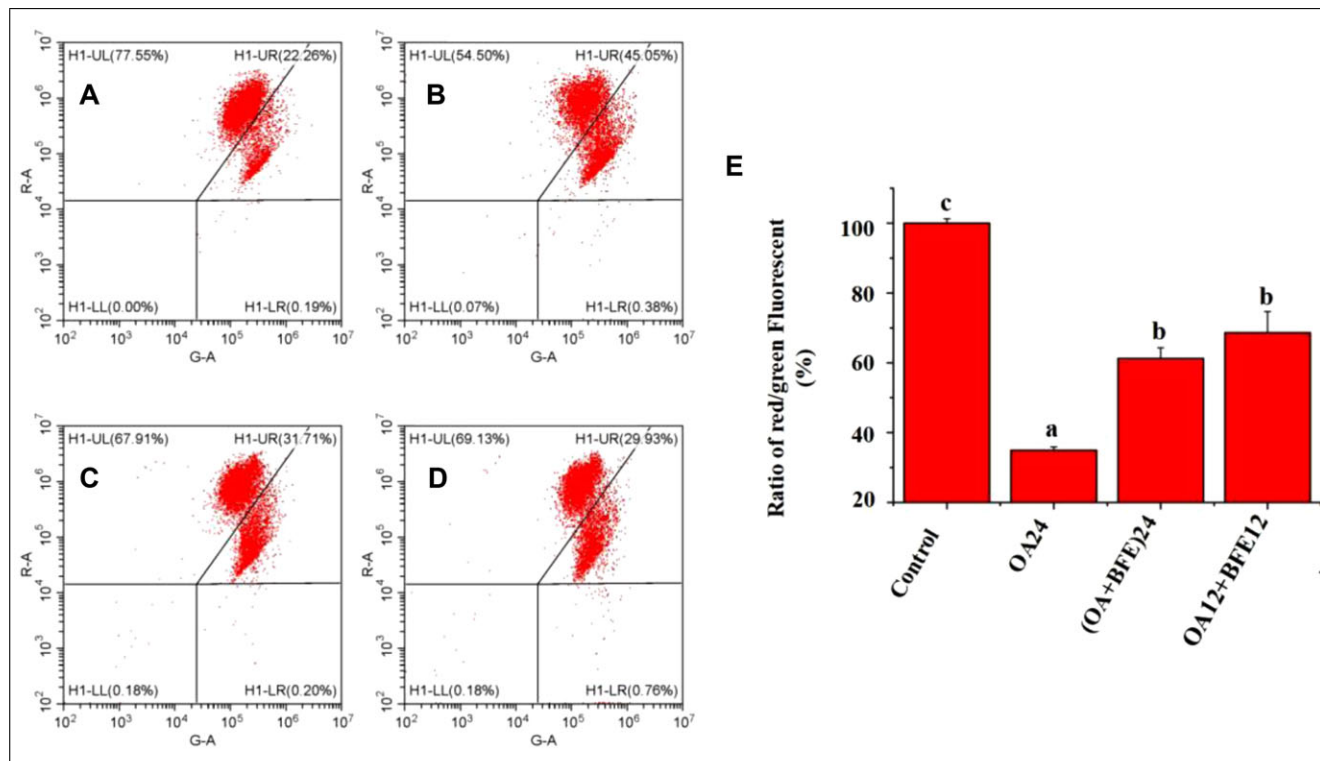


Figure 6—JC-1 staining was used to detect mitochondrial membrane potential levels for the treatments, control group (A), OA24 group (B), (OA+BFE)24 group (C), and OA12+BFE12 group (D). The ratio of red/green fluorescent positive cells was shown for mitochondrial membrane potential levels (E) and the control group was set as 100%. Letters a to c represented the significant difference ( $P < 0.05$ ).

OA24, (OA+BFE)24, and OA12+BFE12 groups were used for the observation. Such parameters, including TG, MDA, LDH, GSH-Px, CAT, T-AOC, ROS production, and mitochondrial membrane potential, were presented for the analysis. As shown in Figure 7A, the top three principal components (PC1, PC2, and PC3) explained 99.47% of the variability by means of log transformation and data centering. Four groups were distributed in different regions and it was also described that there was a tendency to cluster between (OA+BFE)24 and OA12+BFE12 groups because of the adjacent distribution (Figure 7A). Also, both (OA+BFE)24 and OA12+BFE12 groups tended to cluster with control samples, which were also proved by cluster analysis (Figure 7B). Obviously, it was observed that there were significant differences between OA samples and other samples due to the different distributed regions, indicating that OA treatment caused the obvious oxidative stress and the BFE intervention produced effective modulation. As reported above, (OA+BFE)24 and OA12+BFE12 groups tended to cluster, indicating the similar performance of oxidative stress alleviation.

#### qRT-PCR analysis

From the principal components analysis and cluster analysis, (OA+BFE)24 and OA12+BFE12 groups tended to cluster, indicating the similar performance of oxidative stress alleviation. Therefore, each group can be selected for qRT-PCR analysis. But beyond that, the T-AOC level of cells consisted of antioxidants enzymes and low-molecular-weight antioxidants (Wang et al., 2013). Because of the highest T-AOC level, (OA+BFE)24 group was chosen for the determination of the related gene expression to show BFE intervention performance.

As shown in Figure 7C, compared with control samples, Nrf2 expression of OA24 samples was decreased significantly ( $P < 0.05$ ). In agreement with the expression of Nrf2, HO-1 and NQO1 expressions were also altered with significant differences when OA and BFE were introduced ( $P < 0.05$ ). It was highlighted that downregulation of Nrf2 expression depressed multiple antioxidant defense responses, thus resulting in ROS increase beyond a threshold that caused cells damage (DeNicola et al., 2011). Antioxidants from antioxidant defense systems sustained cell proliferation and cell survival signaling resulting in an antioxidant capacity improvement to counteract the increase in ROS production (Tong, Chuang, Wu, & Zuo, 2015). When cells were treated with BFE solution, Nrf2, HO-1, and NQO1 expressions were dramatically activated ( $P < 0.05$ ). The systemic activation also contributed to other antioxidant enzymes motivation, including CAT, GSH-Px, and T-AOC production (Suzuki et al., 2017; Tuzcu et al., 2017; Yu et al., 2014.). Also, TG, LDH, and MDA production was effectively decreased (Figure 3). Altogether, upregulation of Nrf2, HO-1, and NQO1 expression improved the antioxidant defense responses, resulting in an antioxidant capacity to alleviate high ROS production.

#### Autophagosomes characterization

As one component of antioxidant and damage repair systems, autophagy contributes to clearing the irreversibly damaged biomolecules (Gerstenmaier et al., 2015). Recently, many studies report that oxidative stress caused by ROS production is the main intracellular signal transducer for sustaining autophagy (Filomeni, De Zio, & Cecconi, 2015). These reports suggest the importance of the autophagy on the sustaining cell proper function as



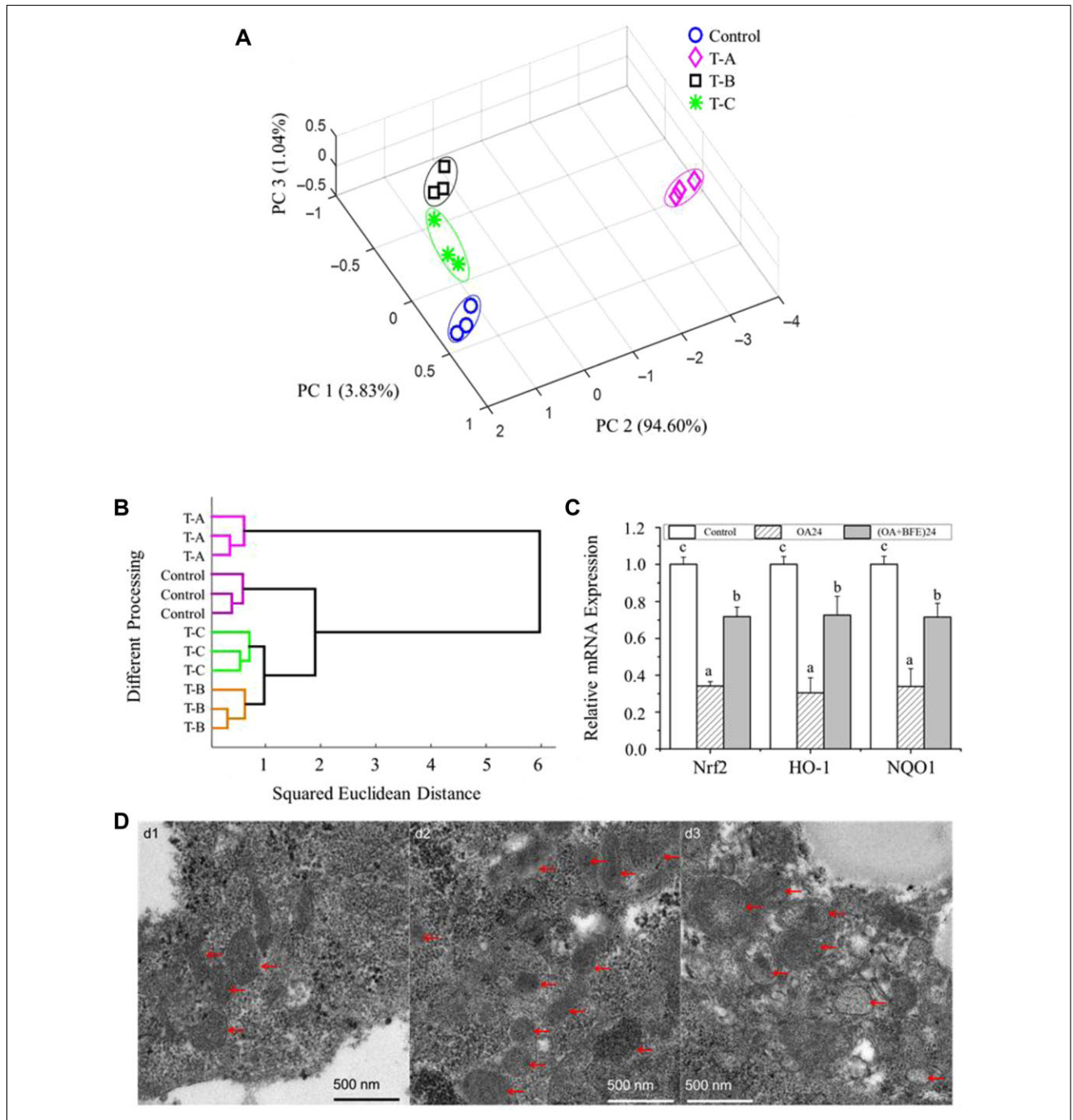


Figure 7—Principal components analysis score plot of the top three principal components (A) and hierarchical cluster analysis (B) of different treatments. T-A, T-B, and T-C represented OA24 group, (OA+BFE)24 group, and OA12+BFE12 group, respectively. qRT-PCR results of the expression of Nrf2, HO-1, and NQO1 (C) regulated by OA and BFE intervention. Letters a to c represented the significant differences ( $P < 0.05$ ). (D) Photos (from transmission electron microscope) of autophagosome for the control group (d1), OA24 group (d2), and (OA+BFE)24 group (d3). Red arrows were used to show the autophagosome and the bar was 500 nm.

one part of antioxidant defense response by negative feedback regulation.

High ROS production could be introduced to initiate autophagy for sustaining proper cell function (Filomeni et al., 2015). Herein, autophagosomes in different groups were described to show the autophagy resulted from OA-induced oxidative stress. Compared with control samples (Figure 7D), the number of autophagosomes of OA24 and (OA+BFE)24 groups was increased

significantly ( $P < 0.05$ ), indicating the autophagy initiation by high ROS production. It was also considered that appropriate ROS production alleviated by BFE intervention reduced the number of autophagosomes.

#### Possible regulatory mechanisms

In particular, high ROS production resulted in cell damage and then decreased Nrf2 expression, and related antioxidant defense

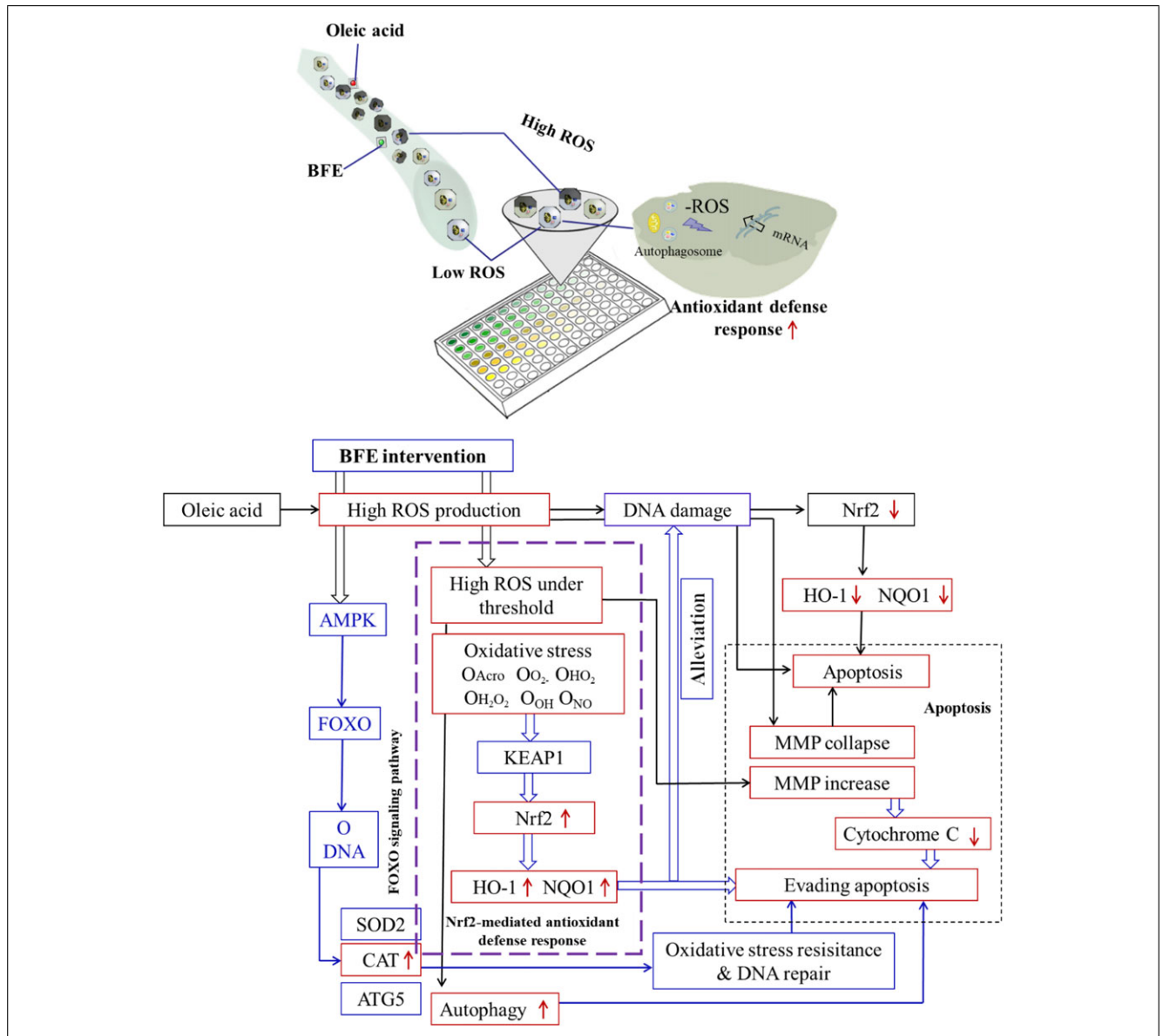


Figure 8—Possible regulatory mechanisms of BFE intervention for oxidative stress alleviation by activating related antioxidant defense responses. Improvement of Nrf2/HO-1/NQO1 expression (purple rectangle) and mitochondrial membrane potential-mediated apoptosis (black rectangle) and FOXO signaling pathway initiation (blue thin arrows) may together contribute to oxidative stress alleviation. Red letters represented the parameters determined in this study. MMP, mitochondrial membrane potential.

responses were depressed (Suzuki & Yamamoto, 2015). The increase in Nrf2 level after BFE intervention in this study subsequently initiated HO-1 and NQO1 expression and together contributed to the antioxidant defense response for cell damage alleviation. In order to better verify the regulatory mechanisms, changes in upstream signaling pathway protein expression, including Nrf2 and HO-1, were evaluated using western blot analysis. As shown in Figure S2, expression of Nrf2 and HO-1 of OA-treated samples decreased ( $P < 0.05$ ), which was in line with the results of mRNA expression (Figure 7C). After the BFE intervention, the expression of Nrf2 and HO-1 increased ( $P < 0.05$ ) along with the improvement of an antioxidant defense response. The results indicated that oxidative stress alleviation induced by BFE intervention was attributed to the upregulated Nrf2/HO-1/NQO1 expression.

In addition, mitochondrial membrane potential-mediated apoptosis pathway and FOXO signaling pathway initiation with the increase in CAT level and autophagy may play a vital role in evading apoptosis (Fang et al., 2016), which was supported by the findings of this study. Herein, possible regulatory mechanisms (Figure 8) were supported by means of KEGG (Kyoto Encyclopedia of Genes and Genomes) database (Chen et al., 2019; Kanehisa et al., 2016) for better understanding of BFE intervention for the alleviation of OA-induced oxidative stress. As shown, BFE intervention improved the expression of Nrf2/HO-1/NQO1 to initiate the antioxidant defense response for counteracting oxidative stress. Moreover, mitochondrial membrane potential and FOXO signaling pathway initiation may also contribute to the oxidative stress alleviation in HepG2 cells.

## Conclusion

To clarify antioxidant BFE intervention for counteracting oxidative stress in HepG2 cells, the cell damage model induced by OA was proposed in this study. Biochemical indexes, intracellular ROS production, lipid droplets accumulation, antioxidant enzymes productions, such as GSH-Px and CAT, and mitochondrial membrane potential were successfully determined to show BFE intervention performance ( $P < 0.05$ ). Importantly, the results of qRT-PCR and western blot determination indicated that BFE intervention upregulated Nrf2/HO-1/NQO1 expression to initiate the antioxidant defense response for counteracting oxidative stress ( $P < 0.05$ ). Moreover, mitochondrial membrane potential-mediated apoptosis and FOXO signaling pathway initiation may together contribute to oxidative stress alleviation in HepG2 cells. Altogether, it was concluded that antioxidant BFE intervention was helpful to recover cell's normal physiological steady state by natural reduction of high ROS production and modulating related antioxidant defense responses.

## Acknowledgments

We acknowledge the support from the Natural Science Foundation of Zhejiang Province, China (Grant No. LQ17C200002) and Public Welfare Project of Huzhou, China (Grant No. 2018GZ28). We also thank the China Scholarship Council (CSC) for the scholarship support.

## Author Contributions

Zhanming Li, Yue Yu, and Hongshun Yang designed the study and interpreted the results. Zhanming Li, Yue Yu, Guangtian Cao, and Shudan Huang collected test data. Zhanming Li and Yue Yu drafted the manuscript. All authors reviewed the manuscript.

## Conflict of Interest

The authors have declared no conflict of interest.

## References

Ayyash, M., Johnson, S. K., Liu, S. Q., Mesmari, N., Dahmani, S., Al-Dhaheri, A., & Kizhakkayil, J. (2018). In vitro investigation of bioactivities of solid-state fermented lupin, quinoa and wheat using *Lactobacillus* spp. *Food Chemistry*, 275, 50–58.

Cao, G., Tao, F., Xin, L., Li, Z., & Zhou, X. (2018). Effects of maternal serine supplementation on high-fat diet-induced oxidative stress and epigenetic changes in promoters of glutathione synthesis-related genes in offspring. *Journal of Functional Foods*, 47, 316–324.

Chandel, N. S. (2015). Evolution of mitochondria as signaling organelles. *Cell metabolism*, 22(2), 204–206.

Chen, L., Tan, G. J. T., Pang, X., Yuan, W., Lai, S., & Yang, H. (2018). Energy regulated nutritive and antioxidant properties during the germination and sprouting of broccoli sprouts (*Brassica oleracea* var. *italica*). *Journal of Agricultural and Food Chemistry*, 66, 6975–6985.

Chen, L., Wu, J. E., Li, Z., Liu, Q., Zhao, X., & Yang, H. (2019). Metabolomic analysis of energy regulated germination and sprouting of organic mung bean (*Vigna radiata*) using NMR spectroscopy. *Food Chemistry*, 286, 87–97.

de Almeida Gonçalves, G., de Sá-Nakanishi, A. B., Comar, J. F., Bracht, L., Dias, M. L., Barros, L., . . . Bracht, A. (2018). Water soluble compounds of *Rosmarinus officinalis* L. improve the oxidative and inflammatory states of rats with adjuvant-induced arthritis. *Food & Function*, 9(4), 2328–2340.

DeNicola, G. M., Karreth, F. A., Humpton, T. J., Gopinathan, A., Wei, C., Frese, K., . . . Calhoun, E. S. (2011). Oncogene-induced Nrf2 transcription promotes ROS detoxification and tumorigenesis. *Nature*, 475(7354), 106–109.

Fang, E. F., Scheibye-Knudsen, M., Chua, K. F., Mattson, M. P., Croteau, D. L., & Bohr, V. A. (2016). Nuclear DNA damage signaling to mitochondria in ageing. *Nature Reviews Molecular Cell Biology*, 17(5), 308–321.

Fatokun, A. A., Tome, M., Smith, R. A., Darlington, L. G., & Stone, T. W. (2015). Protection by the flavonoids quercetin and luteolin against peroxide- or menadione-induced oxidative stress in MC3T3-E1 osteoblast cells. *Natural Product Research*, 29(12), 1127–1132.

Ferlazzo, N., Cirmi, S., Russo, M., Trapasso, E., Ursino, M. R., Lombardo, G. E., . . . Navarra, M. (2016). NF- $\kappa$ B mediates the antiproliferative and proapoptotic effects of bergamot juice in HepG2 cells. *Life Sciences*, 146, 81–91.

Filomeni, G., De Zio, D., & Cecconi, F. (2015). Oxidative stress and autophagy: The clash between damage and metabolic needs. *Cell Death and Differentiation*, 22(3), 377–388.

National Health Commission of China. 2014. *Food additive: Bamboo leaf antioxidant extracts*. Patent (Chinese) No. GB (30615-2014). Beijing, China: Author.

Gerstenmaier, L., Pilla, R., Herrmann, L., Herrmann, H., Prado, M., Villafano, G. J., . . . King, J. S. (2015). The autophagic machinery ensures nonlytic transmission of mycobacteria. *Proceedings of the National Academy of Sciences*, 112(7), E687–E692.

Girgih, A. T., He, R., Hasan, F. M., Udenigwe, C. C., Gill, T. A., & Aluko, R. E. (2015). Evaluation of the in vitro antioxidant properties of a cod (*Gadus morhua*) protein hydrolysate and peptide fractions. *Food Chemistry*, 173, 652–659.

Girish, T. K., Kumar, K. A., & Prasad Rao, U. J. S. (2016). C-Glycosylated flavonoids from black gram husk: Protection against DNA and erythrocytes from oxidative damage and their cytotoxic effect on HeLa cells. *Toxicology Reports*, 3, 652–663.

Gong, J., Xia, D., Huang, J., Ge, Q., Mao, J., Liu, S., & Zhang, Y. (2014). Functional components of bamboo shavings and bamboo leaf extracts and their antioxidant activities in vitro. *Journal of Medicinal Food*, 18(4), 453–459.

Jaja-Chimedza, A., Zhang, L., Wolff, K., Graf, B. L., Kuhn, P., Moskal, K., . . . Raskin, I. (2018). A dietary isothiocyanate-enriched moringa (*Moringa oleifera*) seed extract improves glucose tolerance in a high-fat-diet mouse model and modulates the gut microbiome. *Journal of Functional Foods*, 47, 376–385.

Kanehisa, M., Furumichi, M., Tanabe, M., Sato, Y., & Morishima, K. (2016). KEGG: New perspectives on genomes, pathways, diseases and drugs. *Nucleic Acids Research*, 45(D1), D353–D361.

Kim, Y. S., Ahn, C. B., & Je, J. Y. (2016). Anti-inflammatory action of high molecular weight *Mytilus edulis* hydrolysates fraction in LPS-induced RAW264. 7 macrophage via NF- $\kappa$ B and MAPK pathways. *Food Chemistry*, 202, 9–14.

Kubben, N., & Misteli, T. (2017). Shared molecular and cellular mechanisms of premature ageing and ageing-associated diseases. *Nature Reviews Molecular Cell Biology*, 18(10), 595–609.

Lee, M. S., Lee, B., Park, K. E., Utsuki, T., Shin, T., Oh, C. W., & Kim, H. R. (2015). Dieckol enhances the expression of antioxidant and detoxifying enzymes by the activation of Nrf2–MAPK signalling pathway in HepG2 cells. *Food Chemistry*, 174, 538–546.

Li, X., Zhao, M., Fan, L., Cao, X., Chen, L., Chen, J., . . . Zhao, L. (2018). Chitobiose alleviates oleic acid-induced lipid accumulation by decreasing fatty acid uptake and triglyceride synthesis in HepG2 cells. *Journal of Functional Foods*, 46, 202–211.

Manach, C., Milenkovic, D., Van de Wiele, T., Rodriguez-Mateos, A., De Roos, B., Garcia-Conesa, M. T., . . . Morand, C. (2017). Addressing the inter-individual variation in response to consumption of plant food bioactives: Towards a better understanding of their role in healthy ageing and cardiometabolic risk reduction. *Molecular Nutrition & Food Research*, 61(6), 1600557.

Martinez-Reyes, I., Diebold, L. P., Kong, H., Schieber, M., Huang, H., Hensley, C. T., . . . Woychik, R. (2016). TCA cycle and mitochondrial membrane potential are necessary for diverse biological functions. *Molecular Cell*, 61(2), 199–209.

Menard, J., Christianson, H. C., Kucharzewska, P., Bourseau-Guilmain, E., Svensson, K. J., Lindqvist, E., . . . Bengzon, J. (2016). Metastasis stimulation by hypoxia and acidosis-induced extracellular lipid uptake is mediated by proteoglycan-dependent endocytosis. *Cancer Research*, 76(16), 4828–4840.

Mittal, M., Siddiqui, M. R., Tran, K., Reddy, S. P., & Malik, A. B. (2014). Reactive oxygen species in inflammation and tissue injury. *Antioxidants & Redox Signaling*, 20(7), 1126–1267.

Nirmala, C., Bisht, M. S., Bajwa, H. K., & Santosh, O. (2018). Bamboo: A rich source of natural antioxidants and its applications in the food and pharmaceutical industry. *Trends in Food Science & Technology*, 77, 91–99.

Nwachukwu, I. D., Udenigwe, C. C., & Aluko, R. E. (2016). Lutein and zeaxanthin: Production technology, bioavailability, mechanisms of action, visual function, and health claim status. *Trends in Food Science & Technology*, 49, 74–84.

Rani, V., Deep, G., Singh, R. K., Palle, K., & Yadav, U. C. (2016). Oxidative stress and metabolic disorders: Pathogenesis and therapeutic strategies. *Life Sciences*, 148, 183–193.

Reichert, K. P., Schettinger, M. R. C., Gutierrez, J. M., Pelinson, L. P., Stefanello, N., Dalenogare, D. P., . . . Morsch, V. M. (2018). Lingonberry extract provides neuroprotection by regulating the purinergic system and reducing oxidative stress in diabetic rats. *Molecular Nutrition & Food Research*, 62(16), e1800050.

Ristow, M. (2014). Unraveling the truth about antioxidants: Mitohormesis explains ROS-induced health benefits. *Nature Medicine*, 20(7), 709–711.

Schieber, M., & Chandel, N. S. (2014). ROS function in redox signaling and oxidative stress. *Current Biology*, 24(10), R453–R462.

Sporn, M. B., & Liby, K. T. (2012). NRF2 and cancer: The good, the bad and the importance of context. *Nature Reviews Cancer*, 12, 564–571.

Suzuki, T., Murakami, S., Biswal, S. S., Sakaguchi, S., Harigae, H., Yamamoto, M., & Motohashi, H. (2017). Systemic activation of NRF2 alleviates lethal autoimmune inflammation in scurfy mice. *Molecular and Cellular Biology*, 37(15), e00063–17. <https://doi.org/10.1128/MCB.00063-17>.

Suzuki, T., & Yamamoto, M. (2015). Molecular basis of the Keap1–Nrf2 system. *Free Radical Biology and Medicine*, 88, 93–100.

Thangaraj, K., & Vaiyapuri, M. (2017). Orientin, a C-glycosyl dietary flavone, suppresses colonic cell proliferation and mitigates NF- $\kappa$ B mediated inflammatory response in 1,2-dimethylhydrazine induced colorectal carcinogenesis. *Biomedicine & Pharmacotherapy*, 96, 1253–1266.

Tong, L., Chuang, C. C., Wu, S., & Zuo, L. (2015). Reactive oxygen species in redox cancer therapy. *Cancer Letters*, 367(1), 18–25.

Tuzcu, M., Orhan, C., Muz, O. E., Sahin, N., Juturu, V., & Sahin, K. (2017). Lutein and zeaxanthin isomers modulates lipid metabolism and the inflammatory state of retina in obesity-induced high-fat diet rodent model. *BMC Ophthalmology*, 17(1), 129.

Wang, G., Zhang, H., Lai, F., & Wu, H. (2016). Germinating peanut (*Arachis hypogaea* L.) seedlings attenuated selenite-induced toxicity by activating the antioxidant enzymes and mediating the ascorbate–glutathione cycle. *Journal of Agricultural and Food Chemistry*, 64(6), 1298–1308.

Wang, H., Liu, Y., Qi, Z., Wang, S., Liu, S., Li, X., . . . Xia, X. (2013). An overview on natural polysaccharides with antioxidant properties. *Current Medicinal Chemistry*, 20(23), 2899–2913.

Wardyn, J. D., Ponsford, A. H., & Sanderson, C. M. (2015). Dissecting molecular cross-talk between Nrf2 and NF- $\kappa$ B response pathways. *Biochemical Society Transactions*, 43(4), 621–626.

West, A. P., & Shadel, G. S. (2017). Mitochondrial DNA in innate immune responses and inflammatory pathology. *Nature Reviews Immunology*, 17(6), 363–375.

Wu, D., Chen, J., Lu, B., Xiong, L., He, Y., & Zhang, Y. (2012). Application of near infrared spectroscopy for the rapid determination of antioxidant activity of bamboo leaf extract. *Food Chemistry*, 135(4), 2147–2156.

- Wu, T., Yang, L., Guo, X., Zhang, M., Liu, R., & Sui, W. (2018). Raspberry anthocyanin consumption prevents diet-induced obesity by alleviating oxidative stress and modulating hepatic lipid metabolism. *Food & Function*, *9*(4), 2112–2120.
- Xu, M., Jin, Z., Peckrul, A., & Chen, B. (2018). Pulse seed germination improves antioxidative activity of phenolic compounds in stripped soybean oil-in-water emulsions. *Food Chemistry*, *250*, 140–147.
- Yang, D., Xie, H., Jia, X., & Wei, X. (2015). Flavonoid C-glycosides from star fruit and their antioxidant activity. *Journal of Functional Foods*, *16*, 204–210.
- Yang, J. H., Choi, M. H., Yang, S. H., Cho, S. S., Park, S. J., Shin, H. J., Ki, S. H. (2017). Potent anti-inflammatory and antiadipogenic properties of bamboo (*sasa coreana nakai*) leaves extract and its major constituent flavonoids. *Journal of Agriculture of Food Chemistry*, *65*, 6665–6673.
- Yuan, L., Wang, J., Xiao, H., Wu, W., Wang, Y., & Liu, X. (2013). MAPK signaling pathways regulate mitochondrial-mediated apoptosis induced by isoorientin in human hepatoblastoma cancer cells. *Food and Chemical Toxicology*, *53*, 62–68.
- Yu, X., Yang, R., Gu, Z., Lai, S., & Yang, H. (2014). Anti-tumor and immunostimulatory functions of two feruloyl oligosaccharides produced from wheat bran and fermented by *Aureobasidium pullulans*. *BioResources*, *9*(4), 6778–6790.
- Zhang, Y., Jiao, J., Liu, C., Wu, X., & Zhang, Y. (2008). Isolation and purification of four flavone C-glycosides from antioxidant of bamboo leaves by macroporous resin column chromatography and preparative high-performance liquid chromatography. *Food Chemistry*, *107*(3), 1326–1336.

## Supporting Information

Additional supporting information may be found online in the Supporting Information section at the end of the article.

**Figure S1.** UPLC analysis of the bamboo leaf flavonoids extracts.

**Figure S2.** Western blot and bar graph for the relative expression of Nrf2, HO-1, and Cyt C of the treated HepG2 cells, including the control, OA24, and (OA+BFE)24 groups.

**Table S1.** Primer sequence of Nrf2, HO-1, and NQO1.